Electron Localization Function Comparative Study of Ground State, Triplet State, Radical Anion, and Cation in Model Carbonyl and Imine Compounds

ISABELLE FOURRÉ, BERNARD SILVI, PATRICK CHAQUIN, ALAIN SEVIN

Laboratoire de Chimie Théorique, Université Pierre et Marie Curie, 4 Place Jussieu, 75252 Paris Cedex 05, France

Received 27 October 1998; accepted 22 January 1999

ABSTRACT: The modifications of bonding in carbonyl and imine compounds upon excitation, electron attachment, and ionization were studied within the framework of the electron localization function (ELF). The topological analysis of ELF allows a partition of the molecular space into regions having a clear chemical meaning: the basins. The electronic populations of the basins associated with bonding and nonbonding character, as well as the basin spin densities, were calculated at the MP2 level of the quantum mechanical calculation. Good agreement was found with the classical view in terms of mesomeric structures corresponding to the dominant localization of electrons contained in frontier molecular orbitals (MOs). The variations of the basins population were compared to the predictions of MO theory. © 1999 John Wiley & Sons, Inc. J Comput Chem 20: 897–910, 1999

Keywords: carbonyl and imine compounds; excitation; electron attachment; ionization; electron localization function; bonding analysis

Introduction

Topological theories of chemical bonds[1–3] attempt to ''provide a mathematical bridge between the chemical intuition and wave mechanics, which may be considered as a theoretical justification of chemical ideas.''[4] Because the chemical bond is not an observable, it is not possible to use the interpretative postulates of quantum mechanics in order to build up a pertinent mathematical model of bonding in molecules. Bader pointed out that the topological analysis of a gradient dynamical system is a mathematical theory enabling us to

Correspondence to: I. Fourré; e-mail: fourre@lct.jussieu.fr

CCC 0192-8651 / 99 / 090897-14

reach this goal.[1] In this approach, a local function, whose definition is consistent with the statistical interpretation of quantum mechanics, is used to generate a vector field through the gradient operation. Once this gradient field is obtained, the topological analysis consists of locating the critical points (the zeros of the gradient) and partitioning the space into basins of attractors. In Bader's theory the electron density function is used as a potential function that yields a partition into atomic basins, providing rigorous definitions of concepts such as *atom in a molecule*, *bond path*, *and chemical structure*. However the electron density gradient field does not provide information on the electron pairing that is the central idea of the valence theory of Lewis.[5] To this aim, Bader et al.[6,7] and MacDougall[8] considered the Laplacian of the electron density but did not fully extend the topological approach to this quantity.[9] More recently, Silvi and Savin showed that the electron localization function (ELF) of Becke and Edgecombe[10] is a good candidate for generating a potential function.[3] This function enables a partition that is consistent with the chemical common sense on bonding, and its topological analysis provides a better insight into some aspects of bonding theory that are not firmly settled on the basis of quantum mechanics. By exploiting the properties of the mathematical model, it is possible to develop a theory of chemical reactions based on catastrophe theory.[11] At the present state of the art, the latter theory only deals with reactions in which the system evolves on the ground state Born–Oppenheimer surface. In this case the evolution of the system is described in terms of nuclear coordinates that form the control space of the dynamical system. Because the variation of the control parameters are continuous, the catastrophe theory can be applied in a rather straightforward fashion. However, phenomena exist for which the control parameters undergo discrete variations. For example, we can mention ionization, electron attachment, and electronic excitation. The goal of this study was to perform a preliminary analysis of the bonding evolution occurring during such processes in order to verify if the topological approach can be applied to such cases and investigate the nature of the provided information. Obviously, other techniques, such as valence bond (VB) and molecular orbital (MO) theories, can be applied to understand these processes and therefore will be considered in this article for the sake of comparison.

The simplest carbonyl compound is formaldehyde, whose photochemistry and photophysics have attracted a great deal of interest. Among the large number of calculations that have been carried out on this system, a few have dealt with local properties, in terms of electronic densities only. However, their purpose was mostly to analyze the contribution of frontier MOs in the ground state (GS)[12] or in various excited electronic states,[13] thus keeping the delocalized point of view of chemical bonding. Streitwieser and Kohler analyzed the $n \rightarrow \pi^*$ transition using contour plots of the projected density differences, defined as the integral of the electronic density differences along a particular axis.[14] Integration of these projected density differences in regions limited by zero contours yields estimates of the change of electron population in a given region. In this work, we studied the changes of population arising upon excitation, ionization, or electron attachment in the basins determined by the ELF analysis, whose chemical meaning were discussed. At each step of this study we tried to connect the information provided by the ELF analysis with the predictions based on MO considerations (about the weakening or strengthening of the bonds), on the one hand, and with the VB description (taking into account the possible resonance structures) on the other hand. The applicability of ELF was also tested in the case of asymetrical systems, such as formaldimine, where selectivity arises for the cleavage of a σ bond adjacent to a π system.[15]

Sketch of Topological Analysis of ELF

The ELF was initially proposed by Becke and Edgecombe as a local measurement of electron pairing.[10] It is defined by eq. (1):

$$\eta(\mathbf{r}) = \frac{1}{1 + \left(D(\mathbf{r})/D_h(\mathbf{r})\right)^2} \tag{1}$$

For a single-determinantal wave function built from Hartree–Fock or Kohn–Sham orbitals φ_i,

$$D(\mathbf{r}) = \sum_i |\nabla\varphi_i|^2 - \frac{1}{4}\frac{|\nabla\rho(\mathbf{r})|^2}{\rho(\mathbf{r})} \tag{2}$$

and

$$D_h(\mathbf{r}) = C_F \rho^{5/3}(\mathbf{r}). \tag{3}$$

Physically, $D(\mathbf{r})$ represents the part of the local kinetic energy due to the Pauli principle.[16,17] It is worth emphasizing that because ELF is predicated

on knowledge of the first-order density matrix, it is not an observable. The D_h term is the Thomas–Fermi kinetic energy density, which can be viewed as a renormalization factor, where C_F is the Fermi constant ($C_F = 2.871$ au). The range of values of ELF is restricted to $0 \leq \eta \leq 1$. Where electrons are alone or form pairs with antiparallel spins, the Pauli repulsion is weak and the excess local kinetic energy is low, which corresponds to ELF values close to 1. Between these antiparallel pair domains the same-spin pair probability is higher, yielding additional local kinetic energy and thus ELF values close to 0. An ELF value of 0.5 corresponds to uniform electron gaslike probability.

The topological analysis of ELF allows a partitioning of the molecular space into basins of attractors (local maxima) having a clear chemical meaning. One distinguishes core basins, which are located around a nucleus, and valence basins which fill the remaining space. Valence basins are characterized by their synaptic order, which is the number of cores to which they are connected. Monosynaptic basins correspond to lone pair regions whereas di- or polysynaptic basins correspond to bonding regions. Following the nomenclature introduced by Savin et al., the basins are labeled $T_{[i]}$ (atom labels).[18] The T denotes the type of basin, C is for core, V is for valence, and i is an optional running argument in the case of multiple attractors related to the same atom(s). This analysis provides a first classification of the bonds: shared electrons interactions (including covalent, dative, and metallic bonds) are characterized by di- or polysynaptic valence basins; interactions with no sharing of electrons (including van der Waals, ionic, and hydrogen bonds) are characterized by the absence of di- or polysynaptic valence basins. Of course, quantitative properties of the bonding can also be obtained with ELF by integrating the related property densities over the basins. For example, the average population of a given basin Ω_A is defined by

$$\langle N \rangle_{\Omega_A} = \int_{\Omega_A} \rho(\mathbf{r})\, d\mathbf{r}, \qquad (4)$$

which is generally not an integer number. For a di- or polysynaptic valence basin it is roughly close to twice the bond order. Alternatively, basin populations allow us to recover the Lewis or VB resonance structures. The integrated spin density is

$$\langle S_z \rangle_{\Omega_A} = \tfrac{1}{2} \int_{\Omega_A} (\rho^{\alpha}(\mathbf{r}) - \rho^{\beta}(\mathbf{r}))\, d\mathbf{r}. \qquad (5)$$

A measure of the mean deviation of the population or, more physically, of the delocalization is given by the variance of the population

$$\sigma^2(\langle N \rangle_{\Omega_A}) = \langle N^2 \rangle_{\Omega_A} - \langle N \rangle^2_{\Omega_A}. \qquad (6)$$

The variance is weak when dealing with core basins, whereas it is larger for the valence ones.

Computational Details and Structural Properties

For the purpose of an ELF comparative study, all the molecular structures were optimized at the MP2 level[19] by using the 6–311G** basis set with the Gaussian 94 software[20] on an IBM 370 workstation. As model carbonyl compounds we chose formaldehyde, acetaldehyde, and acetone. Optimized structures of these molecules in their ground electronic state are presented in Figure 1. When dealing with acetone, we constrained the molecule to adopt a C_{2v} symmetry for the sake of a simpler description of electronic properties. The energies of the first vertical triplet state (VT), as well as those of the vertical radical anion (VA) and radical cation (VC), are reported. The relaxed structures of the triplet excited state and the radical anion of each carbonyl compound are both pyramidal. They are displayed in Figures 2 and 3. We restricted ourselves to the relaxed radical cation H_2CO^+, whose structure is displayed in Figure 1(a) (consider the numbers in parentheses). As a representative member of the imine model systems we chose the 2-iminopropane molecule, whose optimized structure is displayed in Figure 4, together with the vertical energies of the first triplet state, anion, and cation species. The wave functions were then computed at the MP2 level[21,22] and used as input for a ''classical'' density analysis (limited to formaldehyde, see next section) and for the ELF analysis (see Results and Discussions). The ELF function analysis and the calculation of the electronic density over the basins were done with the TopMod series of programs developed in our laboratory.[23]

Simplified Description of Bonding in Carbonyl Compound: Acetone Molecule

Immense domains of synthesis, photochemistry, and radical chemistry deal with carbonyl compounds and, in all cases, the electronic properties

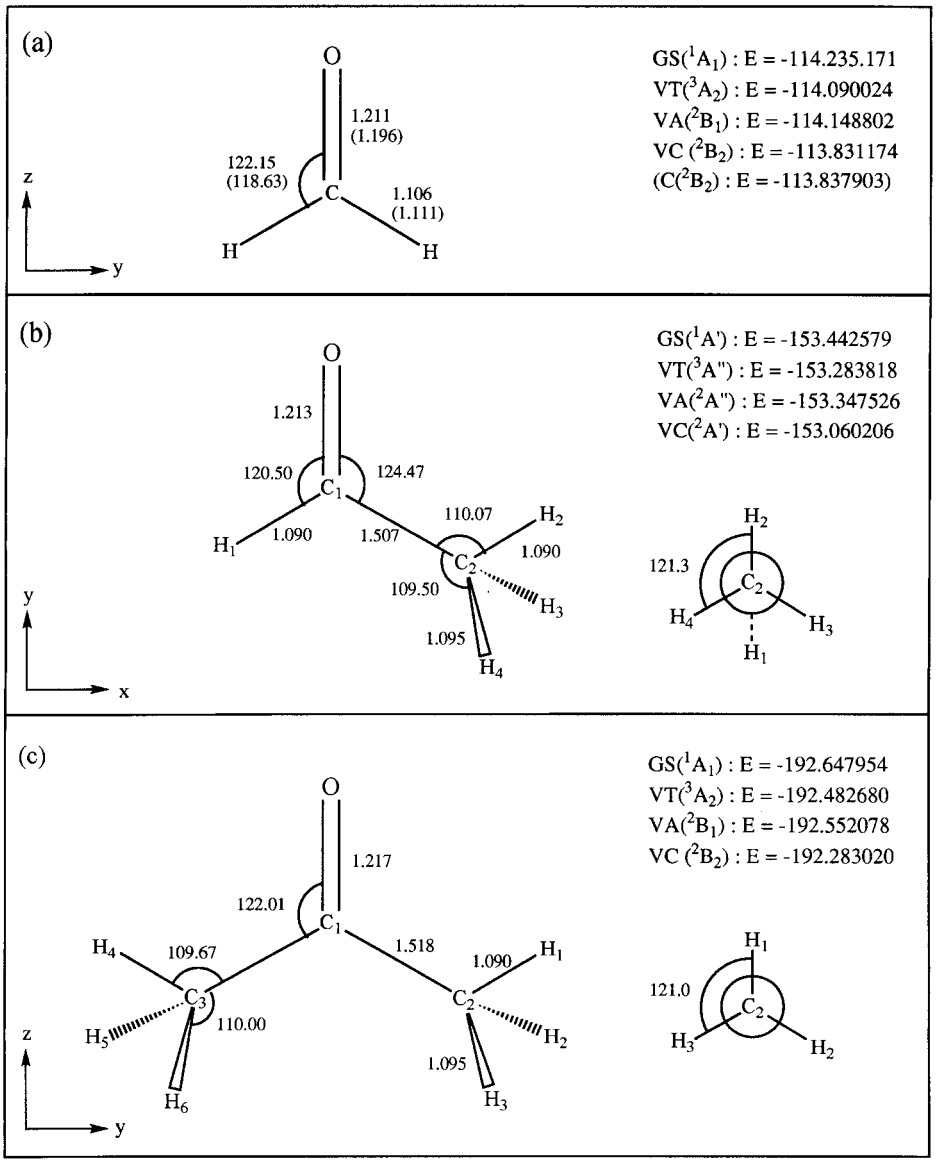

FIGURE 1. Optimized geometry and energy of the ground state (GS) of the carbonyl compounds, as well as the vertical energies of the first triplet state (VT), the radical anions (VA), and cations (VC), at the MP2/6−311G** level: (a) formaldehyde (numbers in parentheses are for the optimized radical cation), (b) acetaldehyde, and (c) acetone. Distances are in Ångstroms, angles are in degrees, and energies are in hartrees.

and reactivity trends have been rationalized in the simple grounds of the limited set of the frontier MOs schematically displayed in the upper part of Figure 5. The dominant electronic features, which have been widely discussed for various low-lying electronic configurations, will be briefly recalled for the sake of comparison with the ELF results. To this aim, we focus our attention on the dominant localization of the electrons, limiting the discussion to vertical states. The topicity terminology will be used for distinguishing the various states under scrutiny in very simple terms.[24]

$^1A_1$ GS

Corresponding to the leading determinant configuration $|(\text{core})(\sigma)^2(\pi)^2(n)^2|$, this state is characterized by four electrons mostly ''localized'' in the molecular plane and two in the perpendicular plane, respectively referred to as σ and π in terms

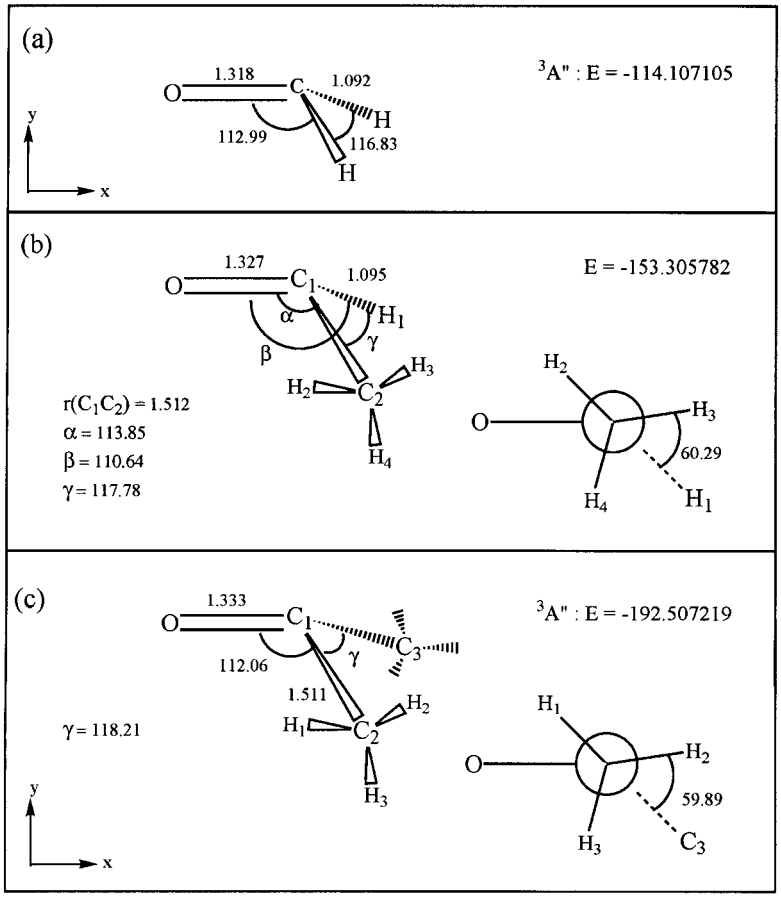

FIGURE 2. Optimized structures (at the MP2/6−311G** level) of the first excited triplet state of (a) formaldehyde, (b) acetaldehyde, and (c) acetone.

of topicity. The associated shorthand notation is $\{4\sigma, 2\pi\}$. It is well known that the actual electronic distribution corresponds to a mixture of the limiting structures **I** and **II** displayed in Figure 5, which is in agreement with the −0.27 and 0.17 charges, respectively, on O and C, calculated at the MP2 level on acetone.

$^3A_2$ TRIPLET STATE

This state, whose leading determinant configuration is $|(\text{core})(\sigma)^2(\pi)^2(n)^1(\pi^*)^1|$, or $\{3\sigma, 3\pi\}$, behaves as a biradical as shown by the MP2-calculated spin densities, which are 1.05 on O and 0.71 on C (same spin). It is noteworthy that both unpaired electrons are localized in orthogonal planes (π for C and σ for O). Due to the removal of one electron from the n MO, the overall polarity is decreased with respect to the GS. No covalent π bond remains; instead a three electrons two centers π bond results as illustrated by the dominant structure **III**. The depletion of population in the n MO has two effects: a decrease of the antibonding character between C and O in the σ plane and a slight decrease of the CH bonding population via the minor contribution of the CH_2 unit. The latter effect plays a leading role in the well-documented Norrish type I reactivity of carbonyl compounds.[25]

$^2B_1$ ANION RADICAL STATE

Its leading determinant configuration is $|(\text{core})(\sigma)^2(\pi)^2(n)^2(\pi^*)^1|$, or $\{4\sigma, 3\pi\}$. The same electronic distribution as in **III** is found in the π plane, thus yielding the dominant structure **IV** in which the spin densities are 0.58 on C and 0.34 on O. The latter result shows that the odd electron is predominantly localized on the C atom with minor contribution on the O according to the resonance scheme

major ↔ minor

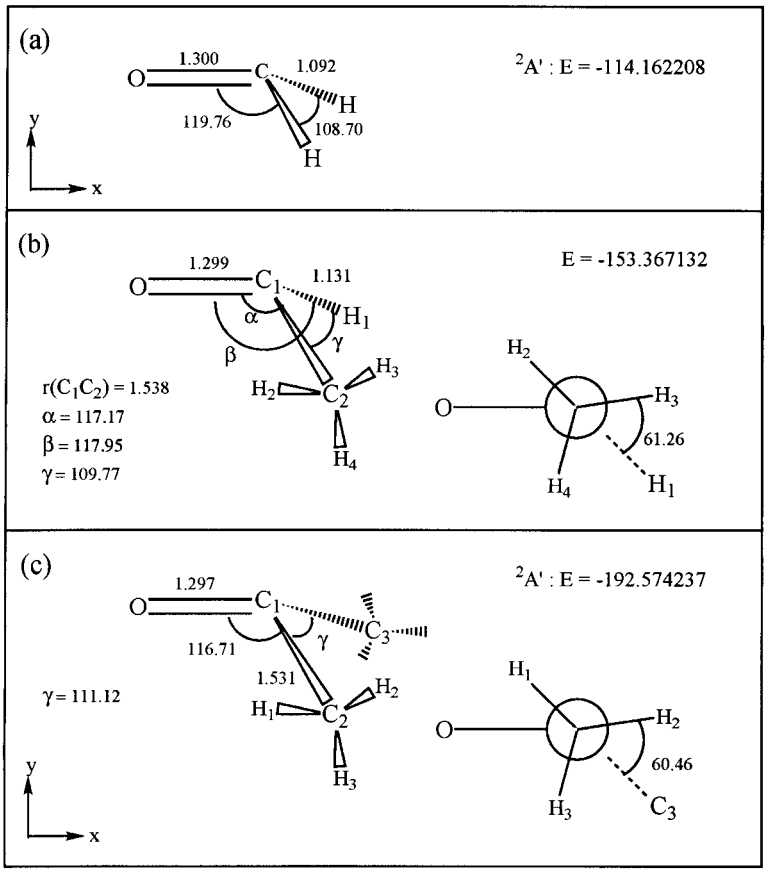

FIGURE 3. Optimized structures (at the MP2/6−311G** level) of the radical anion of (a) formadehyde, (b) acetaldehyde, and (c) acetone.

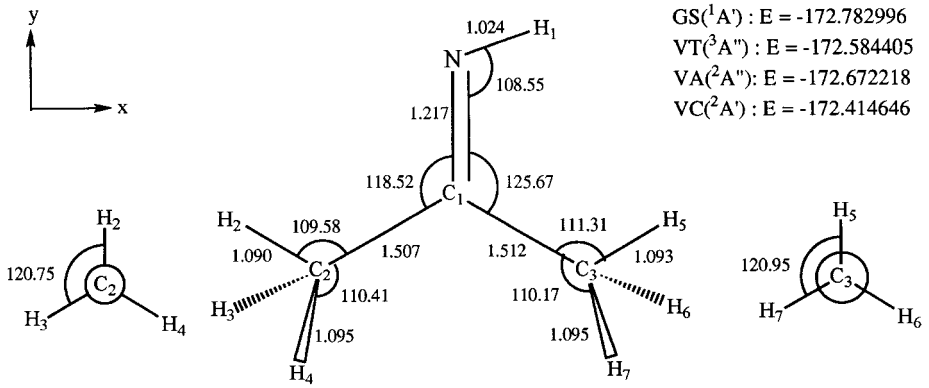

FIGURE 4. Optimized geometry and energy (at the MP2/6−311G** level) of the ground state (GS) of the 2-iminopropane molecule, as well as the energies of the vertical states (VT, VA, VC) (see also Fig. 1).

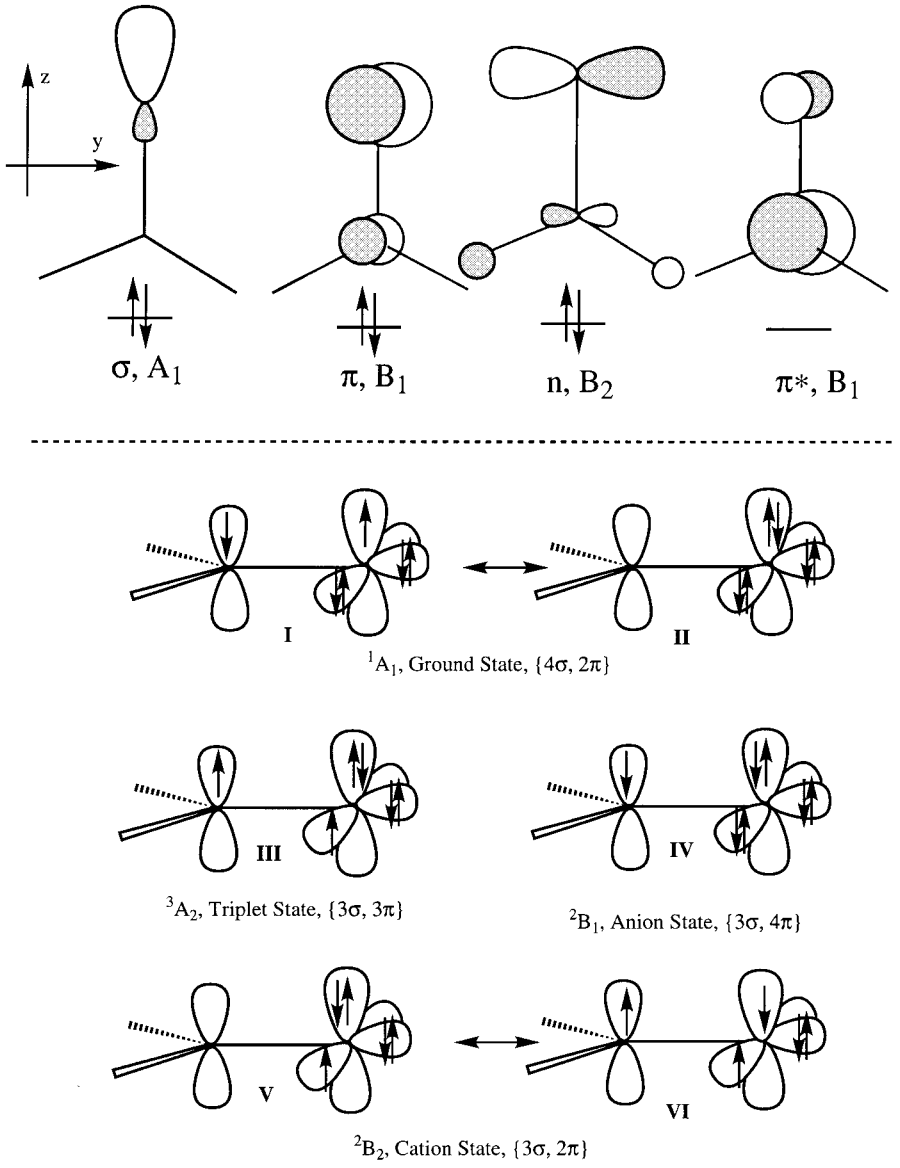

FIGURE 5. In the upper part there is a simple orbital diagram for acetone in its ground state, showing schematic representations of the MOs (the energy increases from left to right). The bottom section shows a schematic representation of the electronic distribution of the states under consideration, in terms of limiting or dominant structures for the ground (**I**–**II**) and the triplet states (**III**), as well as for the ground state of the radical anion (**IV**) and cation (**V**–**VI**).

$^2B_2$ CATION RADICAL STATE

Its leading determinant configuration is $|(\text{core})(\sigma)^2(\pi)^2(n)^1|$, or $\{3\sigma, 2\pi\}$. The same electronic distribution as in the GS is found in the π plane, thus yielding a mixture of limiting structures **V** and **VI**. The oxygen atom bears a strong radical character and a spin density of 0.89, while the carbon atom becomes positive with a 0.20 charge.

In all cases we checked that the electronic trends displayed in structures **III**–**V**, which correspond to vertical states, are accentuated upon structure relaxation in such a fashion that these qualitative results might be safely used in further discussion.

It is noteworthy that the bond length modifications upon relaxation assess these electronic trends.

Results and Discussion

ELECTRON LOCALIZATION IN CARBONYL COMPOUNDS

Prior to going into the details of ELF analysis, it is worth mentioning that the C(O) and C(C) core basins populations, as well as the V(C, H) valence basins populations of methyl substituents, are not (or little) perturbed by the various processes upon investigation. These populations are given in Table I for acetone for the ground and vertical states and for the pyramidal relaxed states. Because in a first step we only consider the vertical transitions, the populations of Table I do not deserve further comment. Thus, we focus our attention on the valence basins that undergo significant modifications [i.e., V(O), $V(O, C_1)$, $V(C_1, H_i)_{i=1,2}$, and (or) $V(C_1, C_i)_{i=2,3}$]. The corresponding MP2 basin populations of the ground state, the first vertical excited triplet state, and the vertical anion and cation of the three carbonyl compounds are given in Table II (see Figs. 1 and 2 for the labeling of atoms). The basin spin densities of the vertical states of acetone are also given. The ELF analysis of the ground state of formaldehyde and the effects of successive substitutions of hydrogen atoms by methyl groups, along the series $H_2CO \rightarrow CH_3CHO \rightarrow CH_3COCH_3$, are presented. The investigation of the vertical states properties allowed us to study the change in electron localization during excitation, ionization, and electron attachment independently of structure relaxation. The consequences of structure relaxation are reported in a later section.

ELF Analysis of GS Valence Basins

H_2CO. The topological analysis of the ELF function gives rise to five valence basins. First, two symmetrical monosynaptic basins $V_i(O)_{i=1,2}$ correspond to the oxygen lone pairs. The location of their attractors is consistent with the VSEPR model.[26] Second, only one disynaptic basin V(O, C) is found. It is associated with the CO bonding region, which confirms that the usual description in terms of σ and π bonds is not supported by ELF. Third, a protonated disynaptic basin V(C, H) is found for each CH bond. At this stage of our study, it is worth comparing the ELF and the Laplacian of the electron density descriptions of the CH bonding. In the former approach the bonded domain is always centered on the proton, while in the latter, according to Bader et al., "... the Laplacian exhibits bonded maxima within the basin of the C atom in addition to the maxima at the position of the proton."[27] In what concerns the basin populations, the $V(O) = V_1(O) \cup V_2(O)$ one at around 4.9 *e* (see Table II) indicates a partial ionic character of the CO bond. On the other hand, the V(O, C) population at around 2.6 *e* is intermediate between that of a simple and a double bond. These results agree with the description given earlier, which essentially consists of the superposition of two limiting structures, an ionic one C^+O^- and a covalent one C=O. The V(C, H) population, although slightly greater than 2 (2.2 *e*), is found at expected values for single bonds.

CH_3CHO. The substitution of a hydrogen atom by a methyl group does not appreciably modify the nature of the chemical bonding in the carbonyl group (see Table II). Nevertheless, as it breaks the molecular symmetry from C_{2v} to C_s, the two oxygen lone pair basins are no longer identical. The V(O) basin populations are reorganized to mini-

TABLE I.
CH_3COCH_3 Molecule.

State	C(O)	$C(C_1)$	$C(C_2)$	$V(C_2, H_1)$	$V(C_2, H_2)$	$V(C_2, H_3)$
GS	2.16	2.10	2.10	1.96	2.02	2.02
VT	2.15	2.11	2.11	1.97	2.03	2.03
VA	2.15	2.11	2.10	2.00	2.05	2.05
VC	2.14	2.09	2.10	1.95	2.00	2.00
T	2.05	2.05	2.10	2.09	2.00	1.91
A	2.07	2.06	2.10	2.04	2.03	2.02

MP2 populations of the core basins and of the protonated valence basins of the methyl groups for the ground state (GS), the first excited triplet state (T), the radical cation (C), and anion (A) [see Fig. 1(c) and 2(c) for the labeling of atoms]. The V prefix takes place for a vertical state.

TABLE II.
MP2 Valence Basin Populations.

State	V(O)	V(O, C)	V(C)	V(H, C)	
			H_2CO		
GS	4.86[a]	2.55		2.17	
VT	4.60[a]	2.08	0.36[a]	2.36	
VA	5.36[a]	1.93	1.14[a]	2.15	
VC	3.71	2.94[a]		2.06	
			CH_3CHO		
State	V(O)	V(O, C_1)	V(C_1)	V(C_1, C_2)	V(H_1, C_1)
GS	4.90[a]	2.58		2.02	2.12
VT	4.60[a]	2.07		1.86	3.03
VA	5.35[a]	1.95	1.27[a]	1.86	2.09
VC	3.90	2.83		1.93	2.02
			CH_3COCH_3		
State	V(O)	V(O, C_1)	V(C_1)	V(C_1, C_2)	
GS	4.88[a]	2.61		2.00	
VT	4.61[a]	2.06	1.06[a]	1.85	
VA	5.33[a]	1.97	1.20[a]	1.92	
VC	3.93	2.83		1.94	
			Basin Spin Densities		
VT	0.40[a]	0.06	0.16[a]	0.10	
VA	0.14[a]	0.02	0.10[a]	0.06	
VC	0.28	0.04		0.04	

The values are for the ground state (GS), the first vertical excited triplet state (VT), and the ground state of the vertical radical anion (VA) and cation (VC) of formaldehyde, acetaldehyde, and acetone. The integrated basin spin densities of the vertical states of acetone, calculated at the B3LYP level, are also given (the missing part is distributed in the remaining basins).

[a] Total population (or spin density) of the equivalent basins related to a same given atom.

mize the Pauli repulsion with the adjacent V(C_1, H_1) and V(C_2, H_2) basins. As the attractor of the latter lies farther from oxygen than that of the former, the population of the basin located on the H_2 side is larger than that of the other by 0.3 *e*. The other effects consist of minor changes in the population of V(O, C_1) (increasing by 0.03 *e*) and in the population of the remaining V(C_1, H_1) (decreasing by 0.05 *e*). The former result is consistent with the slight electron-donor character of the CH_3 group; the latter indicates that the presence of the methyl group makes the C_1H_1 bond itself less of an electron acceptor. The V(C_1, H_1) population still remains greater than the V(C_1, C_2) one; its population of 2 *e* is what one expects for a single bond.

CH_3COCH_3. The substitution of H atoms of H_2CO by two CH_3 groups restores the C_{2v} symmetry and thus the equality of the V_i(O) basins population. The V(O, C_1) population, still increasing by 0.03 *e*, seems to obey an additivity rule upon the H → CH_3 substitution, but the change is not significant. This is in agreement with the known fact that the enhanced electrophilic reactivity of acetaldehyde with respect to acetone is not due to electronic effects but rather to kinetic properties associated with less steric hindrance. The ELF distribution in the acetone molecule, taken as a model for carbonyl compounds, is displayed in the form of a contour map of $\eta(\mathbf{r})$ in Figure 6. In all the contour maps, values of $\eta(\mathbf{r}) > 0.5$ are denoted by a solid contour and those with $\eta(\mathbf{r}) \leq 0.5$ by dotted contours; the solid contours denote a localization greater than that for a uniform electron gas with an identical spin density.[27] All preceding remarks concerning the number, location, and nature of the valence basins can thus be checked. In particular, it exhibits the main characteristics of the monosynaptic V_i(O) basins (oriented as predicted by the VSEPR model), the specificity of the protonated disynaptic basins (which contain the protons), and the propensity of the CO bond for being a double bond [see the oblong shape of the V(O, C_1) basin compared to the V(C_1, C_2) one, oriented perpendicularly with respect to the carbon atoms plane].

Investigation of Vertical States: Acetone

In this section, the modifications of the valence basin populations upon vertical excitation, electron attachment, and ionization processes are analyzed for acetone (see Table II). For the open-shell states, the bonding can also be characterized by the basin spin densities, which are also discussed. Similar trends were found for formaldehyde or acetaldehyde.*

Triplet State. With respect to the GS, the most noticeable change concerns the decrease of the V(O, C_1) population (by 20%): this trend can be

* The only significant differences arise from the presence of protonated valence basins adjacent to the carbonyl bond, whose populations are unexpectedly large, especially in the triplet state; these discrepancies disappear when dealing with the relaxed states.

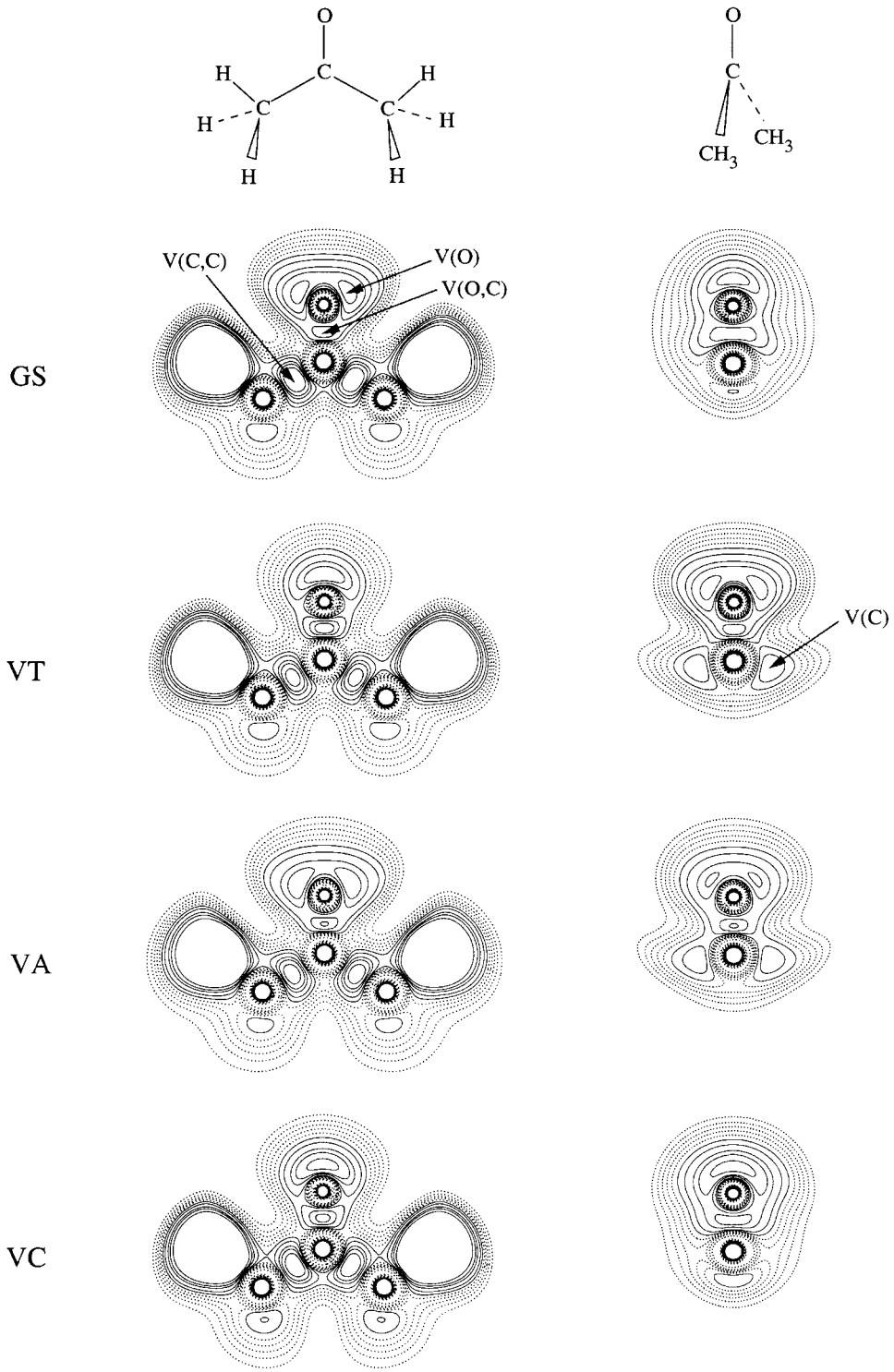

FIGURE 6. Contour plot of $\eta(\mathbf{r})$ for CH_3COCH_3 in its ground (GS) and vertical states (VT, triplet; VA, radical anion; VC, radical cation). The left panels are for the plane of the carbon atoms; the right panels are for the perpendicular plane containing the C–O axis. The first dotted contour adjacent to a solid contour has a value of 0.5 and decrease in steps of 0.1 away from the solid contours. The values of the solid contours are 0.6, 0.7, 0.8, 0.85, and 0.9. The arrows indicate the attractors of the valence basins under scrutiny.

related to the breaking of the covalent π bond, which was predicted in the framework of the MO theory. The decrease of the $V(C_1, C_2)$ population (by around 7%) is consistent with the expected weakening of the σ bond adjacent to a π bond in the course of the $n \rightarrow \pi^*$ transition. The V(O) population also decreases (by around 6%), although remaining greater than 4 *e*. These losses of electron population are compensated by concomitant creation of two new equivalent monosynaptic basins on the adjacent carbon $V_i(C_1)_{i=1,2}$, whose total electronic population amounts to 1.1 *e*. From the basin spin densities also displayed in Table II, one observes that the localization of both odd electrons mostly arises in the lone pairs of O (40%) and to a lesser extent in $V(C_1)$ (16%). Once the contributions of $V(C_1, C_2)$ and $V(C_1, C_3)$ are added to the one of $V(C_1)$, a good agreement is found with the Mulliken atomic spin densities.[†] All these features qualitatively agree with the dominant structure **III** given in Figure 5 and also reflect the diradical nature of this triplet state. Moreover, the comparison of ELF distributions in the GS and in the triplet state (VT) illustrates the modifications in orientation and shape of the bonded and nonbonded valence basins (see Fig. 6). The rotation of the $V_i(O)$ basins from the carbon atoms plane (σ plane) to the perpendicular π plane is clearly seen. Independent of electron population arguments, the shape of the CO bonded domain characterizes a single bond and the contraction of the $V(C_1, C_2)$ basin can be related to the weakening of the associated σ covalent bond. The location of the $V_i(C_1)$ basins on each side of the σ plane is as expected for symmetry reasons.

Radical Anion. With the exception of the two $V_i(O)$ basins, where most of the excess of negative charge is located, the repartitioning of the electronic density among valence basins is similar to that of the triplet state. A more detailed analysis indicates a greater decrease of the $V(C_1, O)$ population bond (by 0.1 *e*) and thus a larger population of the $V(C_1)$ basins than in the triplet state (corresponding to an enhancement of the electron localization on the atoms). Again, the basin spin densities show that the odd electron is predominantly localized into the nonbonded basins, the contribution of the oxygen lone pairs being slightly greater than that of the $V(C_1)$ basins. The contribution of the bonding regions is even less than in the triplet state. Adding the contribution of $V(C_1, C_i)_{i=2,3}$ to the $V_i(C_1)_{i=1,2}$ ones gives rise to the resonance scheme recalled earlier. The ELF distribution (see Fig. 6) illustrates the similarity of the valence basins in the anion (VA) and the neutral (GS) in the σ plane (compare left panels) and in the anion and the triplet (VT) in the π plane (compare right panels) where a part of the excess electron is localized. The spatial arrangement of the oxygen lone pairs domain (see the most inner contour, corresponding to $\eta = 0.9$) results from the repulsion between the V(O) and the $V(C_1)$ basins. Indeed, because the V(O) population is close to that of three lone pairs, one would have expected, for a rather large value of η (here 0.9), to observe a torus shape basin (i.e., two inner identical contours). Actually, there is a thinning of the torus in the π plane, attributed to the previously mentioned interaction. Consequently, the ELF method of analysis provides a reliable theoretical basis for interpreting the VSEPR empirical model.

Radical Cation. Upon ionization, the GS electron localization is modified in such a way that $CH_3COCH_3^+$ possesses only one V(O) basin, which contains approximately one electron less than the corresponding lone pair domains of the neutral molecule. The $V(O, C_1)$ population increases by 0.22 *e*, whereas the $V(C_1, C_2)$ one decreases by 0.06 *e*. This ELF description of ionization is in qualitative agreement with the decrease of antibonding character in the *n* MO along the CO bond (in the σ plane) and the concomitant loss of bonding character along the C_1C_2 bond. Moreover, the radical character is mainly borne by the lone pair of oxygen with an integrated spin density of 0.28. (The Mulliken analysis gives rise to an oxygen spin density of 0.44.) The repartitioning of the electronic density between the carbonyl group valence basins shows that the $C_1{=}O^+$ bond is partly ionic, in agreement with the resonance scheme displayed in Figure 5, which involves both limiting structures **V** and **VI**. The ELF distribution of $CH_3COCH_3^+$ (see Fig. 6) clearly illustrates the unicity of the V(O) basin, as well as the the extension of the $V(O, C_1)$ basins in the σ plane, compared to that of the neutral species. The similarity of the cation and triplet state ELF distributions in the σ plane is not surprising, because of a similar dominant localization of the frontier electrons in the π plane.

[†] The spin densities of Mulliken should be divided by 2 for the sake of comparison.

Investigation of Relaxed States: Acetone

It is interesting to examine how the topological analysis of the ELF function is modified when excited or ionized structures are allowed to relax. When dealing with the triplet and the radical anion states, we restrict our discussion to the case of acetone (see the related part of Table III).

Triplet State. The full geometry optimization [see Fig. 2(c)] has several dramatic consequences on the topological analysis of the ELF function. First, due to the change from C_{2v} to C_s symmetry, only one $V(C_1)$ basin is found on the pyramidalized carbon, so as to minimize the electronic repulsion with the V(O) basin. This is illustrated by the contour plot of the ELF distribution shown in Figure 7. Second, the comparison of Tables II and III shows a significant transfer of population from the $V(O, C_1)$ basin (by about 0.4 *e*) to the V(O) ones (increasing by about 0.6 *e*), which can be related to the stretching of the C_1O bond. Indeed, we recover the empirical inverse relation between the variations of bond order (represented here by the basin population) and bond distance. In contrast, the $V(C_1)$ and $V(C_1, C_2)$ populations are not modified (C_1C_2 bond distance does not vary). Although the population of the C(O) and $C(C_1)$ core basins remains constant in the case of vertical excitation, it decreases upon structure optimization (see Table I) in such a way that the total electronic charge is preserved. In summary, structure optimization results in a more pronounced decrease of the $V(O, C_1)$ population such that this basin has *lost exactly one electron* with respect to the GS. The basin spin densities reflect the enhancement of localization of both odd electrons into the V(O) and $V(C_1)$ monosynaptic basins, mainly due to a transfer from the $V(C_1, C_2)$ and $V(C_1, C_3)$ disynaptic basins. The agreement between this ELF analysis and the dominant mesomeric structure **III** of Figure 5 is better than in the case of the vertical states.

TABLE III.
MP2 Valence Basin Populations.

State	V(O)	V(O, C)	V(C)	V(H, C)	
			H_2CO		
T	5.07*	1.68	1.01		
A	5.82*	1.67	1.19	2.00	
C	3.64	3.00*		2.05	
			CH_3CHO		
State	V(O)	$V(O, C_1)$	$V(C_1)$	$V(C_1, C_2)$	$V(H_1, C_1)$
A	5.14*	1.51	1.07	1.86	2.09
T	5.83*	1.51	1.22	1.92	2.13
			CH_3COCH_3		
State	V(O)	$V(O, C_1)$	$V(C_1)$	$V(C_1, C_2)$	
T	5.22*	1.63	1.07	1.85	
A	5.85*	1.63	1.21	1.89	
			Basin spin densities		
T	0.44*	0.05	0.22	0.07	
A	0.14*	0.01	0.17	0.04	

The values are for the relaxed triplet state (T) and the relaxed radical anion (A) of formaldehyde, acetaldehyde, and acetone. The radical cation case is illustrated by H_2CO^+ (see also caption of Table II).

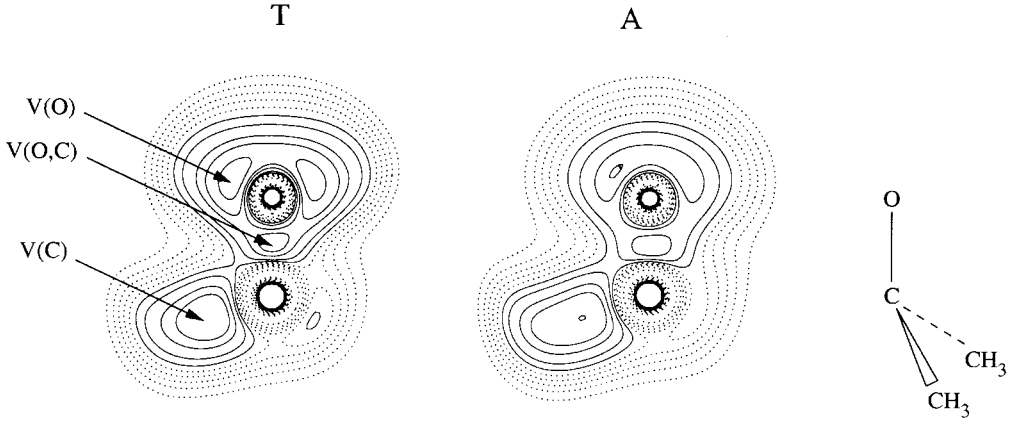

FIGURE 7. Contour plots of $\eta(\mathbf{r})$ for the first excited triplet state of acetone (T) and the ground state of the associated radical anion (A). The contours are represented for the symmetry plane of the (pyramidal) molecules (see also Fig. 6).

Radical Anion. The aforementioned similarity between the nature of the chemical bonding in the VT states and in the VAs is even more pronounced when relaxed states are considered. Besides the similarity of the relaxed structures, the equality of the $V(O, C_1)$ populations (see Table III) confirms that the odd electron, mostly localized in the V(O) basins, has little influence on the overall CO bonding. Indeed, all remarks about the transfers of population or spin densities upon optimization of the triplet are valid for the anion as well. The variations of the basin populations between the relaxed anion and the GS of the neutral [i.e., V(O): 1 *e*; $V(C_1)$: ≈ 1 *e*; $V(O,C_1)$: -1 *e*] are noteworthy. Interesting connections can thus be made with the MO description of the bonding.

Radical Cation. Associated with the shortening of the C_1O bond distance, a decrease of the $V(O, C_1)$ population is actually observed. As an example, in H_2CO^+ there is a transfer of 0.1 *e* from V(O) to V(O, C). Once again the inverse relation between the variations of bond order and bond distance is noteworthy.

IMINE MODEL SYSTEMS

In symmetrical carbonyl compounds, such as acetone, the removal of one electron from the *n* orbital (upon excitation to the π^* orbital or upon ionization) or the addition of one electron (formation of an anion radical) have the same effect on both adjacent bonds to the CO group. If the oxygen atom is replaced by an NH group, the lone pair no longer possesses an in-plane symmetrical arrangement. In addition to modifications of the valence basins populations, a selectivity problem arises: which adjacent bond preferentially weakens in the course of the aforementioned processes, potentially leading to a selectivity in the σ cleavage? The $n \rightarrow \pi^*$ excitation was investigated by Bigot et al. in the framework of Mulliken population analysis.[15] They found that the anti bond (with respect to the lone pair) is weaker than the syn one, the weakening being more pronounced in the $n\pi^*$ state than in the GS. Thus, it was interesting to investigate the ability of ELF to take this selectivity into account.

Table IV shows the valence basins populations of the 2-iminopropane molecule. Following the method used for carbonyl type compounds, we discuss the basin populations of the C=NH group, which appears to be instructive for the understanding of bonding. As expected, the imino group

TABLE IV.
MP2 Valence Basin Populations.

State	V(N)	$V(N, C_1)$	$V(C_1, C_2)$	$V(C_1, C_3)$	$V(C_1)$	$V(H_1, N)$
GS	2.50	3.02*	2.04	2.03		2.04
VT	2.80*	1.99	1.95	1.84	1.11*	1.90
VA	3.15	2.23	2.00	1.88	1.20*	2.00
VC		4.62*	2.03	1.97		2.11

The values are for the 2-iminopropane molecule for the ground state (GS) and the vertical states (see also Table II).

basin populations [$V(N, C_1) = 3.0$ *e* and $V(N) = 2.5$ *e* in the GS] reflect a more covalent character of the N=C linkage than when dealing with the C=O linkage. Other indications of this covalent character enhancement are, on one hand, the greater value of the ELF at the attractor of the $V(N, C_1)$ basin (0.90), than at the V(O, C) one (0.85), and, on the other hand, the existence of two $V(N, C_1)$ basins compared to one V(O, C). For the same reason, the decrease of the $V(N, C_1)$ population following excitation (30%) or formation of anions (25%) is more important than in carbonyl compounds. The radical cation reveals the unexpected absence of a V(N) basin, although only one electron has been removed from the *n* orbital. Nevertheless, we observed that the $V(N, C_1)$ basin spreads in a region that was previously occupied by the lone pair. This may be viewed as another manifestation of the enhancement of covalency with respect to CO. Concerning the weakening of the adjacent $(C_1C_i)_{i=2,3}$ bonds, the selectivity arises very clearly in the excited state, as well as in the radical aniom, and to a lesser extent in the radical cation. The anti $V(C_1, C_3)$ basin population does preferentially decrease, indicating a more important delocalization of the electron between the $V(N, C_1)$ and the anti $V(C_1, C_3)$ basin than between the $V(N, C_1)$ and the syn $V(C_1, C_2)$ basin.

Conclusion

The results presented in this article demonstrate that our ELF-based topological description of the chemical bond provides a deeper insight into the bonding evolution upon excitation, ionization, and electron attachment in carbonyl and imine compounds than the classical MO point of view. The changes occurring in the valence basin populations are, on the one hand, consistent with the findings of the classical descriptions in terms of delocalized MOs or resonance structures and, on the other

hand, provide a chemical picture of the electron cloud reorganization. The integrated spin densities clearly show that the unpaired electron(s) is (are) mostly localized in the monosynaptic (lone pair) basins. The localization of the spin density in the lone pair regions seems to be a general trend already observed in calculations of radicals such as monochlorine oxides, ClO_n.[28] It is noteworthy that this tendency can be somehow hampered by constraints (vertical processes), whose removal (relaxation) enables the spin density transfer from bonding to nonbonding regions. Further work is in progress to interprete the preceding features within the catastrophe theory framework.

References

1. Bader, R. F. W. Atoms in Molecules: A Quantum Theory; Oxford University Press: Oxford, UK, 1990.
2. Gadre, S. R.; Sears, S. B.; Chakravorty, S. J.; Bendale, R. D. Phys Rev 1985, A32, 2602.
3. Silvi, B.; Savin, A. Nature 1994, 371, 683.
4. Aslangul, C.; Constanciel, R.; Daudel, R.; Kottis, P. In Advances in Quantum Chemistry; Löwdin, P.-O., Ed.; Academic Press: New York, 1972; Vol. 6, pp 93–141.
5. Lewis, G. N. Valence and the Structure of Atoms and Molecules; Dover: New York, 1966.
6. Bader, R. F. W.; MacDougall, P. J.; Lau, C. D. H. J Am Chem Soc 1984, 106, 1594.
7. Bader, R. F. W.; Gillespie, R. J.; MacDougall, P. J. J Am Chem Soc 1988, 110, 7329.
8. MacDougall, P. J. Ph.D. Thesis, McMaster University, Hamilton, Ontario, Canada, February 1989.
9. Bader, R. F. W.; MacDougall, P. J. J Am Chem Soc 1985, 107, 6788.
10. Becke, A. D.; Edgecombe, K. E. J Chem Phys 1990, 92, 5397.
11. Krokidis, X.; Noury, S.; Silvi, B. J Phys Chem A 1997, 101, 7277.
12. Dunning, T. H.; Winter, N. W. J Chem Phys 1971, 55, 3360.
13. Buenker, R. J.; Peyerimhoff, S. D. J Chem Phys 1970, 53, 1368.
14. Streitwieser, A.; Kohler, B. J Am Chem Soc 1988, 110, 3769.
15. Bigot, B.; Devaquet, A.; Sevin, A. J.C.S Faraday II 1980, 76, 1234.
16. Tal, Y.; Bader, R. F. W. Int J Quantum Chem 1978, S12, 153.
17. Savin, A.; Jepsen, O.; Flad, J.; Andersen, O. K.; Priess, H.; von Schnering, H. G. Angew Chem Int Ed Engl 1992, 31, 187.
18. Savin, A.; Silvi, B.; Colonna, F. Can J Chem 1996, 74, 1088.
19. Møller, C.; Plesset, M. S. Phys Rev 1934, 46, 618.
20. Frisch, M. J.; Trucks, G. W.; Schlegel, H. B.; Gill, P. M. W.; Johnson, B. G.; Robb, M. A.; Cheeseman, J. R.; Keith, T.; Petersson, G. A.; Montgomery, J. A.; Raghavachari, K.; Al-Laham, M. A.; Zakrzewski, V. G.; Ortiz, J. V.; Foresman, J. B.; Cioslowski, J.; Stefanov, B. B.; Nanayakkara, A.; Challacombe, M.; Peng, C. Y.; Ayala, P. Y.; Chen, W.; Wong, M. W.; Andres, J. L.; Replogle, E. S.; Gomperts, R.; Martin, R. L.; Fox, D. J.; Binkley, J. S.; Defrees, D. J.; Baker, J.; Stewart, J. P.; Head–Gordon, M.; Gonzalez, C.; Pople, J. A. Gaussian 94, Revision D.4, Gaussian Inc.: Pittsburgh, PA, 1995.
21. Lee, C.; Yang, W.; Parr, R. G. Phys Rev 1988, B37, 785.
22. Becke, A. D. J Chem Phys 1993, 98, 5648.
23. Noury, S.; Krokidis, X.; Fuster, F.; Silvi, B. TopMod Package; available at http://www.lct.jussieu.fr/silvi 1997.
24. Dauben, W. G.; Salem, L.; Turro, N. J. Accounts Chem Res 1975, 8, 41.
25. Turro, N. J. Modern Molecular Photochemistry; Benjamin/Cummings; Menlo Park, CA, 1978.
26. Gillespie, R. J.; Robinson, E. A. Angew Chem Int Ed Engl 1996, 35, 495.
27. Bader, R. F. W.; Johnson, S.; Tang, T.-H.; Popelier, P. L. A. J Phys Chem 1996, 100, 15398.
28. Beltrán, A.; Andrés, J.; Noury, S.; Silvi, B. J Phys Chem 1999, in press.